

CO₂ partial pressure and CO₂ emission along the lower Red River (Vietnam)

Thi Phuong Quynh Le^{1*}, Cyril Marchand^{2,3}, Cuong Tu Ho⁴, Nhu Da Le¹, Thi Thuy Duong⁴, XiXi Lu⁵, Phuong Kieu Doan¹, Trung Kien Nguyen⁴, Thi Mai Huong Nguyen¹ and Duy An Vu¹

¹: Institute of Natural Product Chemistry, Vietnam Academy of Science and Technology, 18 Hoang Quoc Viet Road, Cau Giay, Hanoi, Vietnam.

²: IMPMC, Institut de Recherche pour le Développement (IRD), UPMC, CNRS, MNHN, Noumea, New Caledonia, France.

³: Faculty of Chemistry, University of Science – VNUHCM, 225 Nguyen Van Cu, Ho Chi Minh City, Vietnam

⁴: Institute of Environmental Technology, Vietnam Academy of Science and Technology, 18 Hoang Quoc Viet Road, Cau Giay, Hanoi, Vietnam.

⁵: Department of Geography, National University of Singapore, Arts Link 1, Singapore 117570, Singapore.

Correspondence to: Thi Phuong Quynh Le (quynhltp@yahoo.com or quynhltp@gmail.com)

Abstract. The Red River (Vietnam) is a representative example of a South-East Asian river system, strongly affected by climate and human activities. This study aims to quantify the spatial and seasonal variability of CO₂ partial pressure and CO₂ emissions of the lower Red River system. Water quality monitoring and riverine *p*CO₂ measurements were carried out for 24h at five stations distributed along the lower Red River system during the dry and the wet seasons. The riverine *p*CO₂ was supersaturated relative to the atmospheric equilibrium (400 ppm), averaging about 1589 ± 43 ppm, resulting in a water–air CO₂ flux of 530.3 ± 16.9 mmol m⁻² d⁻¹ for the lower Red River. *p*CO₂ and CO₂ outgassing rates were characterized by significant spatial variations along this system, with the highest values measured at Hoa Binh station, located downstream of the Hoa Binh Dam, on the Da River. Seasonal *p*CO₂ and CO₂ outgassing rate variations were also observed, with higher values measured during the wet season at almost all sites. The higher river discharges, enhanced external inputs of organic matters from watersheds and direct inputs of CO₂ from soils or wetland were responsible for higher *p*CO₂ and CO₂ outgassing rates. The difference of *p*CO₂ between the day time and the night time was not significant, suggesting weak photosynthesis processes in the water column of the Red River due to its high sediment load.

Keywords: carbon, human activities, natural condition, *p*CO₂, Red River, Vietnam

35 **1 Introduction**

36 Natural hydrological processes and biogeochemistry of many rivers in the world have suffered from the
37 influences of climate change and human activities in their drainage basins. Riverine carbon fluxes and
38 outgassing are important parts of the carbon exchange among terrestrial, oceanic and atmospheric
39 environment. Rivers and streams not only transfer various forms of carbon (dissolved and particulate)
40 to oceans, but also evade a significant amount of carbon to the atmosphere (Battin et al., 2009; Richey
41 et al., 2002). Due to CO₂ evasion, the flux of carbon that leaves the terrestrial biosphere through global
42 fluvial network was suggested to be twice larger than the amount that ultimately reaches the coastal
43 ocean (Bauer et al., 2013; Regnier et al., 2013). Raymond et al. (2013) estimated a global evasion rate
44 of 2.1 Pg C yr⁻¹ from inland waters, and that global hot spots in stream and rivers which occupy only
45 20 % of the global land surface represented 70 % of the emission. They emphasised that further studies
46 are needed for identifying the mechanisms controlling CO₂ evasion at a global scale.

47 Riverine carbon concentrations and CO₂ outgassing from rivers are impacted by both natural
48 and human factors (Liu et al., 2016; Liu et al., 2017). Recently, spatial and temporal dynamics of *p*CO₂
49 and CO₂ outgassing of Asian rivers are attracting the attention of scientists. Studies of *p*CO₂ and CO₂
50 outgassing from the large Southeast Asian rivers are crucial to quantify geochemical cycles accurately
51 in the context of global changes because the river water discharge, suspended solids and
52 biogeochemical cycles of these rivers have been altered dramatically over the past decades as a result
53 of reservoir impoundment, land use, population, and climate changes (Walling and Fang, 2003; 2006;
54 Lu, 2004). Solid sediment loads not only directly contribute to increase the organic carbon content, but
55 also affect chemical weathering and hence carbon consumption and possible *p*CO₂ (Ran et al., 2015b).
56 Some studies emphasized that data concerning CO₂ outgassing of Southeast Asian rivers is a high
57 priority in order to improve the global evasion rate from inland waters (Raymond et al., 2013;
58 Lauerward et al., 2015).

59 The Red River, with a basin area of 156,450 km², is a typical East Asia river that is strongly
60 affected by climate and human activities. Previous studies reported the hydrology and suspended
61 sediment load associated to some elements loads (N, P, C) of the Red River (Dang et al., 2010; Lu et
62 al., 2015; Le et al., 2015). Recently, the transfer of organic carbon of the Red River to ocean has been
63 studied (Dang et al., 2010; Le et al., 2017). However, there is a lack of data concerning CO₂ outgassing
64 and carbon budget of the lower Red River (Trinh et al., 2012, Nguyen et al., 2018).

65 Consequently, the objectives of this study were: i) to investigate spatial and temporal
66 (seasonal and diurnal) variations of CO₂ partial pressure (*p*CO₂) and CO₂ fluxes at the water-air surface
67 of the lower Red River; and ii) to identify some of the factors that may control *p*CO₂ and CO₂
68 outgassing rates in this system. To our knowledge, our study introduced the first measurement and
69 estimation of CO₂ evasion from the lower Red River.

70 **2 Methods**

71 **2.1 Study sites**

72 The five stations were studied along the lower Red River (Vietnam): Yen Bai station (at the outlet of
73 the Thao River); Hoa Binh station (after Son La and Hoa Binh reservoirs, at the outlet of the Da River);
74 Vu Quang (at the outlet of the Lo River); Hanoi and Ba Lat stations (in the main course of the Red
75 River downstream). The three stations Yen Bai, Vu Quang and Hoa Binh are representative for water
76 quality of the three main tributaries (Thao, Da and Lo) of the upstream Red River, whereas the Hanoi
77 station is representative for the main course Red River after confluence of three main tributaries. Only
78 the Ba Lat station, which is located at the Red River mouth (about 13 km from the sea) is influenced by
79 seawater intrusion (Fig 1). A more detailed description of the river characteristics of the Thao, Da, Lo
80 and the main branch of the Red River can be found in Le et al. (2007).

81 The climate in the Red River basin is tropical East Asia monsoon type, and is controlled by
82 the North East monsoon in winter and South West monsoon in summer. It is, thus, characterized by
83 two distinct seasons: rainy and dry seasons. The rainy season lasts from May to October and cumulates
84 85 – 90 % of the total annual rainfall in the Red River catchment, whereas the dry season covers the
85 period from November to next April. The monsoon climate weather results in a hydrologic regime
86 characterized by large runoffs during the wet season and low runoffs during the dry season (Table 1).

87 A series of dams-reservoirs were impounded in both Chinese and Vietnamese territories of the
88 Red River upstream part (Le et al., 2017). In the Da River, two large dams Hoa Binh and Son La were
89 constructed in the river main course, whereas in the Lo River, two large dams Thac Ba and Tuyen
90 Quang were constructed in its tributaries.

91 The upstream part of the Red River in the Chinese part is dominated by mountain areas, which
92 are tectonically active and unstable, and this, combined with intense rainfall, causes high erosion rates
93 (Fullen et al., 1998), whereas in the Vietnamese part, soils are mostly (70 %) grey and alluvial soils (Le
94 et al., 2017). The Delta is located in a very flat and low land, with an elevation ranging from 0.4 to 12
95 m above sea level (Nguyen Ngoc Sinh et al., 1995). Previous studies showed the difference of lithology
96 in the three upstream tributaries: Paleozoic sedimentary rocks (55.5%), Mesozoic silicic rocks (18.0%)
97 and Mesozoic carbonated rocks (16.7%) dominate in the Thao basin, whereas Paleozoic sedimentary
98 rocks (85.3%) and Mesozoic carbonated rocks (14.7%) cover the Da river basin, and the Lo is
99 composed of Mesozoic silicic rocks (21.5%) and Paleozoic sedimentary rocks (72.7%) (Le et al., 2007;
100 Moon et al., 2007). The delta area is mostly covered by alluvial deposits (80%).

101 Land use was quite different in the three upstream river basins Thao, Da and Lo: industrial
102 crops dominate (58 %) in the Lo basin, forests (70 %) in the Da basin, and paddy rice fields (66 %) in
103 the delta area. The Thao basin is characterized by a larger diversity of land use including forest, paddy
104 rice fields, and industrial crops (85 %) (Le et al., 2015).

105 Population density varied from the upstream to the downstream part of the Red River basin.
106 The delta area, where the Hanoi and Ba Lat stations are located, is characterized by high population
107 density ($> 1,000$ inhabitants km^{-2}). In the upstream part, where the Yen Bai station (in Thao River),
108 Hoa Binh station (in Da River) and Vu Quang station (in Lo River) situate, population density was
109 much lower, about 100 inhabitants km^{-2} (Le et al., 2015).

110 2.2 Sampling procedures and analysis

111 Sampling campaigns were conducted in September (the rainy season) and November (the dry season)
112 2014 at the five gauging stations: Yen Bai, Hoa Binh, Vu Quang, Hanoi and Ba Lat.

113 Physico-chemical parameters were automatically recorded every minute during 24h for each
114 sampling campaign: pH, turbidity, salinity, chlorophyll *a* by a YSI6920 multi-parameters probe (YSI,
115 USA); temperature and dissolved oxygen (DO) by a HOBO sensor (USA). These sensors have been
116 calibrated with suitable standard solutions before each measurement campaign: pH electrode
117 (YSI6920) was calibrated using standard solutions (pH = 4.01 and pH = 6.88, Merck) and the pH
118 precision and accuracy was ± 0.01 ; DO electrode was calibrated using the saturated $\text{Na}_2\text{S}_2\text{O}_3$ solution
119 (Japan) and the DO accuracy was 0.1.

120 In parallel of in-situ measurement, river water samples were hourly collected for analysis of
121 other water quality variables (TSS, DOC, POC, and total alkalinity) during 24h. A known volume of
122 well-mixed sample was filtered immediately by vacuum filtration through pre-combusted (at 450°C for
123 6 h) glass fiber filters (Whatman GF/F, 47 mm diameter). The filters were then kept in a freezer (-20
124 $^\circ\text{C}$) until analysis of TSS and POC. For the measurement of TSS, each filter was dried for 1h at 105°C
125 and then weighed. Taking into account the filtered volume, the increase in weight of the filter
126 represented the total TSS per unit volume (mg L^{-1}).

127 POC concentrations were estimated on the same filters. Filters were then weighed before and
128 after calcination at 550°C for 4 hours. The difference in weight before and after calcination was
129 multiplied by 0.4 to provide an estimation of the POC content (Servais et al., 1995).

130 A volume of 30 ml sub-sample of filtrate was acidified with $35\ \mu\text{l}$ 85 % H_3PO_4 acid and then
131 stored at 4°C in amber glass bottles until measurement of the DOC concentrations using a TOC- V_E
132 (Shimadzu, Japan). The samples, standards and blank measurements were measured in triplicate and
133 the analytical error was below 3 %.

134 Total alkalinity of the hourly samples was immediately determined on non-filtered water
135 samples (30 ml water sample) in situ by titration method with 0.01M HCl (APHA, 1995). For each
136 sample, triplicates were titrated and the analytical error was below 3 %.

137 2.3 Hydrological data collection

138 Daily and hourly data of river water discharges in 2014 at the 5 hydrological stations studied were
139 collected from the Vietnam Ministry of Natural Resources and Environment (MONRE, 2014). The
140 daily data were collected for all days in 2014 (Figure SM1), whereas hourly data were obtained for the
141 exact dates of field measurements at the 5 sites (Table 1). The mean annual river flows in 2014 of the
142 Thao, Da, Lo Rivers and in the main axe of the Red River at the Hanoi and Ba Lat stations were: $527 \pm$
143 515 ; 1369 ± 833 ; 1302 ± 517 ; 1867 ± 1089 ; $615 \pm 293\ \text{m}^3\ \text{s}^{-1}$, respectively. Higher values of river
144 discharges were observed in wet season (May to October) than in dry season (January-April;
145 November-December) at all sites (Table 1).

146 Water velocity at the 5 sites varied from $0.3\ \text{m s}^{-1}$ at Vu Quang site in the dry season to $1.0\ \text{m}$
147 s^{-1} at Hoa Binh and Yen Bai sites in the wet season. The mean water depth varied with the highest

148 values recorded at the Vu Quang Site in the rainy season and the lowest at Ba Lat estuary in both the
149 rainy and the dry seasons (Table 1).

150 **2.4 $p\text{CO}_2$ determination**

151 $p\text{CO}_2$ in the water column was measured using an equilibrator connected to a portable infrared gas
152 analyser (IRGA), and also calculated using T_{alk} and pH measured in-situ.

153 **2.4.1 Measured $p\text{CO}_2$**

154 An equilibrator was used to determine the $p\text{CO}_2$ in water equilibrated with the air. The equilibrator was
155 designed, as described in Frankignoulle et al. (2001), as follow: a vertical plastic tube (height: 73 cm,
156 diameter: 9 cm), which is filled up with about 250 glass marbles (diameter = 1.5 cm) in order to
157 increase the surface exchange between water and air. The river water (water inlet) through a submerged
158 pump at 20 cm below the river surface water comes into the equilibrator from the top of the tube. The
159 water inlet can be regulated by a flow controller installed under the tygon tubing, which joins the water
160 inlet with the pump. A closed air circuit ensures circulation through the equilibrator (from the bottom
161 to the top), a water trap, a particle filter, a flow regulator and a portable infrared gas analyser (IRGA)
162 (Licor 820, Licor[®], USA), which was calibrated before each sampling campaign using a series of
163 standards concentrations of 0, 551 and 2756 ppm CO_2 (Air Liquide[®]). The IRGA was connected to a
164 computer interface, which allows recording the $p\text{CO}_2$ every second. Values were recorded during 24 h
165 continuously. The accuracy is <3% of reading.

166 **2.4.2 Calculated $p\text{CO}_2$**

167 DIC content may be calculated from the sum of total dissolved inorganic carbon in water including
168 HCO_3^- , CO_3^{2-} , H_2CO_3 and CO_2 , or can be calculated from a combination of any two of the following
169 measured parameters total alkalinity, pH, or partial pressure of CO_2 ($p\text{CO}_2$) (Park, 1969). In this study,
170 DIC contents were calculated from the sum of including HCO_3^- , CO_3^{2-} , H_2CO_3 and CO_2 contents,
171 which were given by the calculation from the CO_2 -SYS EXCEL Macro Software (version 2.0) based
172 on the total alkalinity contents and pH values measured in-situ as described above (Sect. 2.3).

173

174 **2.5 CO_2 fluxes determination**

175 The water-air CO_2 fluxes from the equilibrator measurement at each site were calculated by the
176 formula proposed by Raymond and Cole (2011) as followings:

$$177 \quad F_{\text{Equi}} = k_{600} * \alpha * (p\text{CO}_2 \text{ water} - p\text{CO}_2 \text{ air}) \quad \text{Eq. (1)}$$

178 Where F is the CO_2 flux from water ($\mu\text{mol m}^{-2} \text{s}^{-1}$) and converted in $\text{mmol m}^{-2} \text{d}^{-1}$;

179 k_{600} , was gas transfer velocity of CO_2 or piston velocity (cm h^{-1}). Some studies indicate that k_{600} values
180 are closely related to flow velocity and channel gradient for rivers (Alin et al., 2011). In this study, k_{600}
181 was calculated using the equation from Raymond et al. (2012) based on stream velocity (V , in m s^{-1}),
182 slope (S , unitless), depth (D , in meters) and discharge (Q , in $\text{m}^3 \text{s}^{-1}$), as follow:

183
$$k_{600} = 4725 \pm 445 \times (V \times S)^{0.86 \pm 0.016} \times Q^{-0.14 \pm 0.012} \times D^{0.66 \pm 0.029} \text{ Eq. (2)}$$

184 α is the solubility coefficient of CO₂ for given temperature and salinity (Weiss, 1974) (mol L⁻¹ atm⁻¹).
185 In this case, $\alpha = 0.034 \text{ mol L}^{-1} \text{ atm}^{-1}$. In this study, salinity variations were low, except for the Ba Lat
186 station. Temperature did not change a lot. We checked the influence of different α values in the dry (α
187 = $3.941 \times 10^{-2} \text{ mol L}^{-1} \text{ atm}^{-1}$ at 24 °C) and the wet season ($\alpha = 3.138 \times 10^{-2} \text{ mol L}^{-1} \text{ atm}^{-1}$ at 27 °C) at the 5
188 sites and compared with the constant α value of $0.034 \text{ mol L}^{-1} \text{ atm}^{-1}$.

189 Both $p\text{CO}_2$ in the water determined from Equilibrator measurement (in ppm) and from
190 CO₂_SYS calculation (in atm) were converted in μmol when calculating the flux of CO₂ outgassing.

191

192 **2.5. Statistical analysis**

193 To detect the correlation between environmental variables and $p\text{CO}_2$, statistical software R version
194 3.3.2 (R Core Team, 2016) was applied to calculate the Pearson correlation coefficients. Some
195 environmental variables were evaluated by “cor” to compare the correlation and selected representative
196 variables. PCA analysis was then used for identifying representative variables that could relate to the
197 dynamic of $p\text{CO}_2$.

198 Student t-test was used to test the difference of variables values between the two different
199 times (the wet and the dry) and (the day and the night), whereas ANOVA was used to test the
200 difference of variables within stations on the measured mean variables. Probabilities (p) were
201 determined and a p value of < 0.05 was considered to be significant.

202

203 **3. Results**

204 **3.1. Physical and chemical variables of the lower Red River**

205 Water temperature varied from 23.3 to 29.4 °C, and the mean value in rainy period (27.4 °C) was higher
206 than the one in dry period (24.5 °C) at almost all stations, except at the Hoa Binh site where the water
207 temperatures did not show seasonal variations, remaining around 26.3 - 26.5 °C. Among the five
208 hydrological stations, the higher water temperatures were recorded at the Hanoi and Ba Lat stations,
209 ranging from 28 to 29 °C in the wet period, whereas they were close to 23 °C during the dry period.
210 Temperatures at the Yen Bai and Vu Quang stations were approximately 26 °C in the wet period and 24
211 °C in the dry period (Table 2). No clear difference for water temperature during the day and at the night
212 time was observed at the 5 sites in both the rainy and the dry season (p < 0.05).

213 pH values were slightly different between the two periods, being higher in the dry season than
214 in the wet season at all the sites (Table 2) (p < 0.05). pH ranged from 7.7 to 8.2 with an average of 8.1
215 for all the sites. The lowest pH values were measured at the Hoa Binh in both periods (< 8), whereas
216 they ranged between 8.0 and 8.4 at the other sites.

217 The percentage of dissolved oxygen (% DO) varied from 50.5 % to 70.7 % with an average
218 value of 64.3 % (Table 2). The mean values were the highest for the Yen Bai station (70.1 %) in the
219 wet period, and 69.5 % for the Ba Lat station in the dry period. The lowest values were observed at the
220 Hoa Binh station in both periods (55.0 % in the wet period, 51.4% in the dry period) (Table 2). DO
221 showed the seasonal and spatial variations but no clear day-night difference was observed ($p < 0.05$).

222 Salinity values at the four upstream sites were under the detection limit both in the rainy and
223 dry seasons, but in the estuary downstream river at the Ba Lat station, values up to 8.75 were measured
224 during the dry season (Table 2). Conductivity followed the same trend as salinity, and was close to
225 $0.2 \pm 0.0 \text{ mS cm}^{-1}$ for the 4 upstream sites, and reached up to $6.6 \pm 3.4 \text{ mS cm}^{-1}$ at Ba Lat (Table 2).

226 Total alkalinity ranged from 84.3 ± 1.9 to $152.9 \pm 6.6 \text{ mg L}^{-1}$, with higher values measured in
227 the dry season than in the rainy season ($p < 0.05$), except at Vu Quang station. The difference of total
228 alkalinity was spatially recorded but no clear variation appeared between values in day and night times
229 at 5 sites ($p < 0.05$).

230 Chlorophyll *a* was quite low during the two sampling campaigns, ranging from 0.23 to 2.77
231 $\mu\text{g L}^{-1}$, with an average of $1.61 \mu\text{g L}^{-1}$. Higher values in the rainy season than in the dry season were
232 observed but no clear day-night difference was observed at almost sites ($p < 0.05$). From Yen Bai to Ba
233 Lat, Chl-*a* concentrations in the main axe (at Yen Bai and Hanoi stations) were higher than in the two
234 tributaries Da and Lo (Table 2), even under the higher values of turbidity.

235 **3.2. Carbon concentrations of the lower Red River**

236 During the two sampling campaigns, DOC concentrations ranged from 0.5 to 4.6 mgC L^{-1} , averaging
237 1.5 mgC L^{-1} . Higher values were observed during the rainy season (2.0 mgC L^{-1} vs. 1.5 mgC L^{-1} during
238 the dry season), and the highest value was recorded at Hanoi station (Table 2). POC concentrations
239 varied from 0.4 to 4.6 mgC L^{-1} . Among the 5 sites, POC concentrations in the main reach of the Red
240 River (Yen Bai, Hanoi and Ba Lat sites) were higher than in the two tributaries Da and Lo, where dams
241 were constructed. Spatial and seasonal variations of DOC and POC were observed but no clear
242 difference in day – night time was found ($p < 0.05$) (Table 2, table SM1).

243 DIC concentrations at the five sites fluctuated between 16.7 and 32.9 mgC L^{-1} , averaging 23.8
244 mgC L^{-1} . Lower values were measured in the rainy season (22.3 mgC L^{-1}) than in the dry season (25.3
245 mgC L^{-1}) and the difference of DIC was noted for the 5 sites ($p < 0.05$) (Table 2).

246

247 **3.3. Comparisons of the $p\text{CO}_2$ results obtained by the two methods**

248 $p\text{CO}_2$ along the lower Red River (Vietnam) in the dry and the wet seasons were determined by two
249 methods: i) direct measurements using an equilibrator connected to an IRGA, ii) calculated from pH
250 and alkalinity using the $\text{CO}_2\text{-SYS}^{\text{®}}$ software. The direct $p\text{CO}_2$ measurements gave slightly higher
251 values than the calculated ones (Table 2), but the values of two methods were similar and presented the

252 same trend of spatial and seasonal variations ($R^2 = 0.77$, Fig. 2; Table 2). Lower values of the
253 calculated $p\text{CO}_2$ in this study may be caused by the analytical errors in pH or under-estimation of total
254 alkalinity. Similarly, the CO_2 outgassing rates which were calculated from measured $p\text{CO}_2$ from
255 equilibrator were higher than the ones derived from the calculated $p\text{CO}_2$ from CO_2 -SYS, however they
256 are in the same orders and have similar variation trends (Table 3, Fig 2).

257 Below, we use the results of $p\text{CO}_2$ (and $f\text{CO}_2$) from direct measurements to discuss the spatial and
258 seasonal variations of $p\text{CO}_2$ (and $f\text{CO}_2$) of the lower Red River.

259 **3.4. Relations between $p\text{CO}_2$ and water chemistry variables**

260 The riverine water $p\text{CO}_2$ was supersaturated with CO_2 in contrast to the atmospheric equilibrium (400
261 ppm), averaging $1,589 \pm 43$ ppm for all sites observed. In general, the results did not show a clear
262 variation in $p\text{CO}_2$ between the day and night, except higher values at the night time at the Ba Lat site
263 and higher value in daytime at Vu Quang in dry season ($p < 0.05$) (Table 2). This leads to the same
264 trends of CO_2 outgassing rates: no clear difference between daytime ($548.9 \pm 17.9 \text{ mmol m}^{-2} \text{ day}^{-1}$) and
265 night time ($551.8 \pm 15.9 \text{ mmol m}^{-2} \text{ day}^{-1}$) ($p < 0.05$) (Table 3, Fig. 3).

266 $p\text{CO}_2$ values fluctuated from 694 ppm (at Yen Bai) in the dry season to 3,887 ppm (at Hoa
267 Binh) in the wet season in 2014. The mean values were the highest for the Hoa Binh station in both
268 seasons whereas the lowest one was observed at the Yen Bai site. Spatial variations of both $p\text{CO}_2$ and
269 $f\text{CO}_2$ flux for all 5 sites were observed ($p < 0.05$). Higher values of $p\text{CO}_2$ in the wet season than in the
270 dry season were observed at almost all the sites ($p < 0.05$) (Table 2).

271 CO_2 outgassing rates of the 5 stations of the lower Red River showed seasonal and spatial
272 variations ($p < 0.05$). The highest value was recorded at Hoa Binh site in both the rainy and the dry
273 season, averaging $1447.5 \pm 27.4 \text{ mmol m}^{-2} \text{ d}^{-1}$ and the lowest value was observed at Ba Lat site,
274 averaging $54.6 \pm 6.5 \text{ mmol m}^{-2} \text{ d}^{-1}$. CO_2 outgassing rates were higher in the wet season than in the dry
275 season at all sites (Table 3, Fig. 3).

276 PCA and Pearson correlation coefficient were performed to analyze the relationships between
277 nine environmental variables and $p\text{CO}_2$ at the five sampling stations of the lower Red River in the wet
278 season (September 2014) and the dry season (November 2014). The PCA of the seasonal data for five
279 sampling stations presented a clear separation between two periods (Fig. 4a). The rainy period was
280 characterized by the factors of flow, temperature, $p\text{CO}_2$, POC, DOC, turbidity and Chl a. The dry
281 season is mainly governed by the factors of DIC, salinity, and conductivity. The spatial differences
282 appeared for almost variables in both wet and dry seasons (Fig. 4b). Among the five stations, the Hoa
283 Binh station is characterized by the $p\text{CO}_2$ and CO_2 flux, whereas the Ba Lat station had strong
284 influences by salinity and conductivity. The other stations showed the combination of different factors.
285 The Hoa Binh station has highest flows that correlate with the $p\text{CO}_2$ and CO_2 flux.

286 The Pearson correlation coefficient showed a strong negative correlation between $p\text{CO}_2$ and
287 pH and oxygen saturation (%) ($r \sim -0.8$ for both). A low positive correlation between $p\text{CO}_2$ and DIC

288 and DOC was found ($r \sim 0.15$) (Table 4). However, the $p\text{CO}_2$ is positively correlated with the flow of
289 the river ($r = 0.3$). Consequently, we included that the $p\text{CO}_2$ are the results of a combination of multiple
290 parameters, rather than a single one, such as the flow of river, season (including precipitation and
291 temperature), dam construction, population density, geomorphological characteristics of the catchment.

292 **4. Discussion**

293

294 **4.1 Temporal variations of $p\text{CO}_2$ and CO_2 fluxes of the lower Red River**

295 Different explanations were given for the day-night variation of $p\text{CO}_2$ and CO_2 flux for aquatic
296 ecosystems in the world. Previous studies indicated that water temperature could alter the riverine
297 $p\text{CO}_2$ value because CO_2 solubility decreases with the temperature increase during the day (Parkin and
298 Kaspar, 2003). This effect was observed for some rivers in the world (Guasch et al., 1998; Dornblaser
299 and Striegl, 2013; Peter et al., 2014). Other study revealed that photosynthesis of phytoplankton may
300 have a strong influence on circadian variation of $p\text{CO}_2$ or CO_2 outgassing, since this process consumes
301 CO_2 during the day (Linn and Doran, 1984).

302 Concerning the lower Red River, water temperature did not show clear variation between the
303 day and the night. In addition, low Chl-a concentrations were measured, from 0.5 to 3.1 $\mu\text{g L}^{-1}$,
304 probably as a result of the high turbidity limiting light penetration in the water column. Thus,
305 phytoplankton activity had a low influence on C dynamic in the lower Red River system.
306 Consequently, there are no clear variations of $p\text{CO}_2$ and CO_2 fluxes between the day and the night time
307 at the different stations along the lower Red River.

308 Regarding seasonal variations, some authors suggested that higher water temperatures in the
309 wet season in tropical regions were responsible for increased $p\text{CO}_2$ and higher CO_2 emissions to the
310 atmosphere (Hope et al., 2004; Li et al., 2012). Dessert et al., (2003) suggested that higher temperature
311 should also induce higher weathering rates, leading to higher DIC export. Increase in temperature
312 decreases CO_2 solubility but increase OM decomposition processes, which produce CO_2 . These
313 processes may partly explain the higher $p\text{CO}_2$ of the lower Red River during the hot and rainy season.
314 However, direct relationship between temperature and $p\text{CO}_2$ was not evidenced during the rainy
315 season, probably because riverine inputs were the dominant factor driving $p\text{CO}_2$. Conversely during the
316 dry season, $p\text{CO}_2$ clearly increased with temperature, suggesting that metabolic rate controlled $p\text{CO}_2$
317 when adjacent soils inputs are limited (Fig. 5).

318 Another important factor that impacted $p\text{CO}_2$ seasonal variations in the lower Red River was
319 the river discharge. Indeed, during the monsoon season, the Red River discharges were about 2 to 3
320 times higher at all the sites ($p < 0.05$) (Table 1). Higher $p\text{CO}_2$ and CO_2 flux values in wet season were
321 observed at almost all sites ($p < 0.05$). CO_2 flux varied from $54.6 \pm 6.5 \text{ mmol m}^{-2} \text{ d}^{-1}$ (at Ba Lat) in the
322 dry season to $1447.5 \pm 27.4 \text{ mmol m}^{-2} \text{ d}^{-1}$ (at Hoa Binh) in the wet season. The higher $p\text{CO}_2$ and CO_2
323 flux values observed during the wet season may reflect the influence of soil organic matter inputs to the
324 riverine water column, evidenced by the higher values of DOC and POC in the rainy seasons measured
325 in our study ($p < 0.05$). In tropical regions, the wet season usually experienced higher $p\text{CO}_2$ than the dry

326 season because the intense rainfall induced higher OM inputs into the river (Richey et al., 2002) or in
327 addition inputs of CO₂ from wetlands. This process was observed in some subtropical rivers: the
328 Longchuan River (Li et al., 2012) and the Xijiang River (Yao et al., 2007), with pCO₂ values
329 increasing significantly when baseflow and interflow increased, and flushed significant amount of
330 carbon into the streams. Other example which could be mentioned is the case of the Godavari River in
331 Indonesia, where extreme high value of pCO₂, up to ~30,000 ppm, were measured probably due to
332 significant organic carbon decomposition during peak discharge period. This was in contrast with the
333 very low values measured (<500 ppm) during the dry season for this river (Sharma et al., 2011).

334 To conclude, no clear day-night time variation of both pCO₂ and fCO₂ at 5 sites of the lower
335 Red River in 2014 was found but our results showed the clear seasonal variation of both pCO₂ and
336 fCO₂. The spatial variation of pCO₂ and fCO₂ at 5 sites of the lower Red River under the natural and
337 anthropogenic factors will be discussed below.

338

339 **4.2 Spatial variations of pCO₂ and fCO₂ outgassing**

340 **4.2.1 Influence of geomorphological characteristics**

341 The upstream of the Red River is located in mountainous areas, where chemical and
342 mechanical erosion are among the world highest (500 mm per 1,000 years) (Meybeck et al., 1989),
343 which may participate in the elevated pCO₂ values measured. The geologic substratum of the upstream
344 Red River is dominated by consolidated paleozoic sedimentary rocks, with variable contributions of
345 mesozoic silicic or carbonate rocks. During rainfall events, the erosion of these rocks may increase
346 pCO₂ in the tributary river waters of the Thao, Da and Lo, which were supersaturated with CO₂ in air
347 from about 2 to 14 times. Our results showed that the pCO₂ mean value of the lower Red River (1589 ±
348 43 ppm) was close to the ones of some Asian rivers such as the downstream Mekong River: 703 – 1597
349 ppm (Alin et al., 2011); the Longchuan River: 2101 – 2601 ppm (Li et al., 2012); the Changjiang
350 River: 1,297 ± 901 ppm (Wang et al., 2007); the Yellow River: 2,811 ± 1,986 ppm (Ran et al., 2015a)
351 (Table 5). However, very high pCO₂ value, up to 11,000 ppm, was also observed for other Asian rivers,
352 like the Xijiang River (Yao et al., 2007).

353 CO₂ emissions from the lower Red River varied in a high range, from 54.6 ± 6.5 to 1447.5 ±
354 27.4 mmol m⁻² d⁻¹, averaging 550.3 ± 16.9 mmol m⁻² d⁻¹. They were close to the values of some large
355 Asian rivers as the Yellow River (856±409 mmol m⁻² d⁻¹) (Ran et al., 2015b) and the Xijiang river (357
356 mmol m⁻² d⁻¹) (Yao et al., 2007) or some rivers in South America reported by Rasera et al. (2013) such
357 as the Negro, the Solimoes, the Caxiuana rivers (855 ± 294, 518 ± 17, 778 ± 17 mmol m⁻² d⁻¹,
358 respectively) (Table 5). Thus, the high alkalinity, pCO₂ and fCO₂ in the Red River in this study can be
359 partly explained by wide distribution of carbonate-silicate rocks in the upper Red River drainage area,
360 especially during high water discharge as observed for other Asian rivers.

361

362 **4.2.2 Influence of hydrological characteristics**

363 Spatially, pCO₂ differences between the three upstream tributaries and the main downstream axe of the
364 Red River are suggested to be partially related to different hydrological characteristics and
365 management of the three sub-basins and delta area, as observed in other systems (Yao et al., 2007; Li et

366 al., 2012). Our results showed that within the 3 upstream sites studied, the highest $p\text{CO}_2$ values were
367 always measured in the Da River at Hoa Binh site, where river discharges were the highest ($2,189 \pm 39$
368 $\text{m}^3 \text{ s}^{-1}$ in the wet season and $868 \pm 319 \text{ m}^3 \text{ s}^{-1}$ in the dry season) ($p < 0.05$), whereas the lowest $p\text{CO}_2$
369 were measured at the Yen Bai station of the Thao River, where river discharges were the lowest ($840 \pm$
370 $68 \text{ m}^3 \text{ s}^{-1}$ in the wet season and $260 \pm 18 \text{ m}^3 \text{ s}^{-1}$ in the dry season) (Table 1 and Table 2). Figure 4
371 showed the clear difference of $p\text{CO}_2$, CO_2 flux and river discharges in the rainy and the dry seasons for
372 the lower Red River.

373 Regarding the Ba Lat site, which is situated in the Red River estuary and thus in a very low
374 and flat land, $p\text{CO}_2$ values were lower than in Hanoi. It is interesting to observe that the river water
375 discharge at Hanoi site ($3,296 \pm 86$ and $1,915 \pm 149 \text{ m}^3 \text{ s}^{-1}$) was about 3 times higher than the one at Ba
376 Lat ($1,269 \pm 93$ and $453 \pm 31 \text{ m}^3 \text{ s}^{-1}$) in both wet and dry seasons respectively (Table 1), whereas higher
377 $p\text{CO}_2$ values were measured during the dry season in Hanoi than in Ba Lat (1,150 and 800 ppm,
378 respectively), but during the rainy season the values were close, i.e. around 1,450 ppm. We think that
379 dilution by seawater may lead to a reduction of riverine surface water $p\text{CO}_2$, especially in the dry
380 season when the river flow was lower ($p < 0.05$). The higher salinity values measured at Ba Lat site in
381 the dry season (3.6) than in the wet season (0.2) may confirm our suggestion that tidal action
382 influenced at Ba Lat site in the Red River estuary. This result is consistent with previous observations
383 in the Changjiang River estuary (Chen et al., 2008; Bai et al., 2015).

384

385 ***4.2.3 Influence of land-use on $p\text{CO}_2$ and CO_2 emissions***

386 Land cover in the river basin may play a considerable role in controlling riverine $p\text{CO}_2$. As known,
387 severe erosion due to sparse vegetation cover may enhance chemical weathering by increasing the
388 exposure surface of fresh minerals to atmosphere (Millot et al., 2002). Li and Bush (2015)
389 demonstrated that deforestation and agricultural expansion in the Mekong River basin accelerated
390 chemical and physical weathering rates, leading to changes in riverine carbon fluxes. In fact, very high
391 $p\text{CO}_2$ values (up to 30,008 ppm) were observed in the Godavari estuary due to large-scale erosion and
392 deforestation in the catchment area, which accelerated the export of organic carbon into the river,
393 especially in wet season (Sharma et al., 2011). In contrast, recently in another study, lower $p\text{CO}_2$ in one
394 sub-basin (HR) than the average of the Yellow River basin was observed because of the development
395 of an alpine meadow ecosystem reducing soil erosion (Ran et al., 2015a). For the Red River, highest
396 riverine $p\text{CO}_2$ and CO_2 flux values were observed in the Da at the Hoa Binh site despite this sub-basin
397 is dominated by forest as its land cover. This may suggest other factors (reservoir impoundment and
398 geological characteristics) which may strongly control $p\text{CO}_2$ and CO_2 flux of the Da River.

399 In addition, agricultural soil in the river basin may have significant impact on riverine $p\text{CO}_2$.
400 A study concerning the long-term variation of $p\text{CO}_2$ of the Yellow River showed that high pH in
401 irrigation water caused the increase in riverine pH, leading to further reducing $p\text{CO}_2$ (Ran et al.,
402 2015a). This agrees with our results for $p\text{CO}_2$ in the Red River when considering the decrease of the
403 $p\text{CO}_2$ values especially in dry season from upstream Delta area at Hanoi ($1,139 \pm 29$ ppm) to the
404 estuary at Ba Lat (mean value of 816 ± 69 ppm) where rice field and irrigation channels are very dense.

405

406 **4.2.4 Influence of dams on $p\text{CO}_2$ and CO_2 emission**

407 Previously, reservoirs were suggested to decrease riverine $p\text{CO}_2$ due to increased residence times and
408 autotrophic production (Wang et al., 2007). However, Lauerward et al., (2015) found a low negative
409 correlation between them. Abril et al., (2005) noted that intense mineralization of organic matter (OM)
410 originating from the reservoir was possibly a significant source for $p\text{CO}_2$ value in downstream river. In
411 addition, the influence of the dam on the gas transfer velocity and then CO_2 outgassing flux in the river
412 downstream of the dam was also demonstrated in the study of the Sinnamary River (Guérin et al.,
413 2007). In the present study, in the upstream part, $p\text{CO}_2$ ranged from 964 ppm (at Yen Bai) to 3,830
414 ppm (at Hoa Binh), being highest at the Hoa Binh site where the lowest pH values were measured.
415 Higher k_{600} values (from 63 to 68 cm h^{-1}) were also observed at the Hoa Binh and Vu Quang sites.
416 Noted that the Hoa Binh site is situated downstream a series of reservoirs, which have been constructed
417 in both Chinese and Vietnamese parts including two large dams Hoa Binh (in 1989) and Son La (in
418 2010). The Vu Quang site is located in the downstream of a series of reservoirs, including two
419 important Thac Ba (in 1970) and Tuyen Quang (in 2010). Previous studies emphasized that these dams
420 have impacted water and sediment discharges downstream (Ha and Vu 2012; Ngo et al. 2014; Lu et al.
421 2015) with significant sediment deposition being observed in the reservoirs (Dang et al. 2010; Vinh et
422 al. 2014; Lu et al. 2015). Thus, the higher $p\text{CO}_2$ measured at these sites (average value of 3129 ± 32
423 ppm) may reflect the increased decomposition of OM and/or the water perturbation due to dam
424 construction, especially for the Da River. The impact of dams on downstream $p\text{CO}_2$ may be less for the
425 Lo and the Thao Rivers (average values of 1395 ± 63 ppm and 993 ± 14 ppm, respectively), where less
426 numbers and less size (only small and medium) of dams/reservoirs were built up in their upstream
427 parts. Thus, the high $p\text{CO}_2$ measured at these stations may reflect the increased decomposition of OM
428 and/or the water perturbation due to the large dam construction.

429

430 **4.2.5 Influence of population density on $p\text{CO}_2$ and CO_2 emission**

431 Previous studies demonstrated very high value of $p\text{CO}_2$ in river estuaries as a result of different human
432 activities. For instance, $p\text{CO}_2$ up to $\sim 25,000$ ppm was measured in the Rhine estuary (Kempe, 1982) or
433 up to $\sim 15,200$ ppm in the Scheldt estuaries due to high discharge of pollutants (Borges and
434 Frankignoulle, 2002).

435 Concerning the Red River, from the upstream to the downstream part of the main axe, $p\text{CO}_2$
436 together with CO_2 outgassing flux slightly increased from Yen Bai (993 ± 14 ppm and 364.9 ± 10.3
437 $\text{mmol m}^{-2} \text{d}^{-1}$ respectively) to Hanoi ($1,275 \pm 17$ ppm and 304 ± 7.3 $\text{mmol m}^{-2} \text{d}^{-1}$), whatever the
438 season. However, it is worth to note that the Hanoi station was located within the city itself and at this
439 station, the river has not yet received the wastewater discharge of the whole city. Consequently, the
440 Hanoi station in this study may not reflect the influence of whole city, with probably lower O_2 and
441 higher $p\text{CO}_2$ levels as observed for other urban rivers in the Red River Delta (Trinh et al., 2007; 2009;
442 2012).

443 Consequently, our results revealed that $p\text{CO}_2$ and CO_2 flux along the lower Red River were
444 spatially different which reflect the influence of both anthropogenic activities (dam, urban effluents),
445 and natural characteristics (rainfall-river discharge, temperature and geology) in the watershed.

446

447 **5. Conclusions**

448 This work presented the spatial and seasonal variability of $p\text{CO}_2$ along the lower Red River system.
449 The riverine water was supersaturated with CO_2 in contrast to the atmospheric equilibrium (400 ppm),
450 with $p\text{CO}_2$ values averaging about 1589 ± 43 ppm, resulting thus in a water–air CO_2 flux of 550.3 ± 16
451 $\text{mmol m}^{-2} \text{d}^{-1}$ from the lower Red River system. The $p\text{CO}_2$ from the water surface of the lower Red
452 River network was characterized by significant spatial variations, being the highest at the Hoa Binh
453 dam downstream and in the main axis at Hanoi station. The highest value obtained at Hoa Binh site may
454 reflect the important impact of a series of large dams (Son La, Hoa Binh) and geomorphological
455 characteristics in the Da River, but also the high water discharge, whereas the high $p\text{CO}_2$ value in
456 Hanoi may partly reflect the influence of population density through the release of organic carbon into
457 the river. The monsoon season resulted in an increased amount of OM inputs from adjacent soil led to
458 higher $p\text{CO}_2$ and CO_2 flux values. Consequently, this study evidenced that $p\text{CO}_2$ and CO_2 flux along the
459 lower Red River were controlled by both anthropogenic activities (dam, urban effluents), and natural
460 characteristics (rainfall-river discharge, temperature and geology) in the watershed. Long-term
461 variations of $p\text{CO}_2$ and CO_2 outgassing flux of the Red River may be performed in a future research
462 effort to contribute to studies of regional and global carbon emission under natural and anthropogenic
463 impacts.

464 **Author contribution**

465 Le TPQ, Marchand C and Ho TC designed the experiments. Le TPQ, Ho TC and Vu DA carried the in-
466 situ experiments. Le TPQ, Le ND and Phuong KD contribute to data treatment and calculations. Le
467 TPQ and Marchand C prepared the manuscript with the contributions from all co-authors.

468 **Acknowledgements**

469 This work was performed in the framework of the *ARCP2014-03CMY-Quynh/ARCP2013-06CMY-*
470 *Quynh/ARCP2012-11MY-Quynh* and the *Vietnam-NAFOSTED 105.09-2012.10* projects. The authors
471 would like to thank the Asia-Pacific Network for Global Change Research (APN) and the Vietnam's
472 National Foundation for Science and Technology Development (NAFOSTED-Vietnam) for their
473 financial supports. We thank Ms Nguyen Bich Ngoc for helping field work for data treatment. We
474 highly appreciate the valuable advices and comments provided by the anonymous reviewers.

475 **References**

476 Abril, G., Guérin, F., Richard, S., Delmas, R., Galy-Lacaux, C., Gosse, P., Tremblay, A., Varfalvy, L.,
477 Dos Santos, M.A, and Matvienko, B.: Carbon dioxide and methane emissions and the carbon
478 budget of a 10-year old tropical reservoir (Petit Saut, French Guiana), *Global Biogeochem. Cycle*.
479 19, GB4007, doi:10.1029/2005GB002457, 2005.

480 Alin, S. R., Fatima, R. M., Salimon, C.I ., Richey, J. E., Krusche, A. V., Holtgrieve G. W., and
481 Snidvongs, A.: Physical controls on carbon dioxide transfer velocity and flux in low-gradient river
482 systems and implications for regional carbon budgets, *J. Geophys. Res.* 116, G0100, 2011.

483 APHA, (American Public Health Association). : Standard Methods for the Examination of Water and
484 Wastewater, American Public Health Association editor, 1995.

485 Araujo, M., Noriega, C., Veleda, D., and Lefevre, N.: Nutrient input and CO₂ flux of a tropical coastal
486 fluvial system with high population density in the northeast region of Brazil, *J. Water Resource*
487 *Prot.*, 5, 362-375, doi: 10.4236/jwarp.2013.53A037, 2013.

488 Battin, T. J., Luysaert, S., Kaplan, L. A., Aufdenkampe, A. K., Richter, A., and Tranvik, L. J.: The
489 boundless carbon cycle, *Nat. Geosci.*, 2, 598-600, 2009.

490 Bauer, J. E., Cai, W.-J., Raymond, P. A., Bianchi, T. S, Hopkinson, C.S. and Regnier, P.A.G.: The
491 changing carbon cycle of the coastal ocean, *Nature*, 504(7478), 61–70, doi: 10.1038/nature12857,
492 2013.

493 Borges, A.V., Djenidi, S., Lacroix, G., Theate, J., Delille B., and Frankignoulle, M.: Atmospheric CO₂
494 flux from mangrove surrounding waters, *Geophys. Res. Lett.*, 30(11), 1558, 2003.

495 Borges, A. V., and Frankignoulle, M.: Distribution and air-water exchange of carbon dioxide in the
496 Scheldt plume off the Belgian coast, *Biogeochem*, 59, 41–67, doi:10.1023/A:1015517428985,
497 2002.

498 Bai, Y., Cai, W.-J., He, X., Zhai, W., Pan, D., Dai, M., and Yu, P.: A mechanistic semi-analytical
499 method for remotely sensing sea surface *p*CO₂ in river-dominated coastal oceans: A case study
500 from the East China Sea, *J. Geophys. Res. Oceans*, 120, 2331– 2349, doi:10.1002/2014JC010632,
501 2015.

502 Cole, J. J., and Caraco, NF.: Carbon in catchments: connecting terrestrial carbon losses with aquatic
503 metabolism, *J. Mar. Freshwater Res.*, 52(1), 101 – 110, 2001.

504 Chen, C.T.A., Zhai, W.D., and Dai, M.: Riverine input and air–sea CO₂ exchanges near the
505 Changjiang (Yangtze River) Estuary: Status quo and implication on possible future changes in
506 metabolic status, *Cont. Shelf Res.*, 28, 1476–1482, 2008.

507 Dang, T.H., Coynel, A., Orange, D., Blanc, G., Etcheber, H., and Le, L.A.: Long-term monitoring
508 (1960–2008) of the river-sediment transport in the Red River Watershed (Vietnam): Temporal
509 variability and dam-reservoir impact, *Sci Total Environ.*, 408, 4654–4664, 2010.

510 Dessert, C., Dupré, B., Gaillardet, J., Francois, L. M., and Allegre, C.J.: Basalt weathering laws and the
511 impact of basalt weathering on the global carbon cycle. *Chem. Geol.*, 202, 257–273, 2003.

512 Dornblaser, M. and Striegl, R.: Seasonal variation in diel carbon dynamics, Beaver Creek, Alaska,
513 AGU Fall Meeting Abstracts, p 15–27, 2013.

514 Dubois, K. D., Lee, D., and Veizer, J.: Isotopic constraints on alkalinity, dissolved organic carbon, and
515 atmospheric carbon dioxide fluxes in the Mississippi River, *J. Geophys. Res.*, 115, G02018,
516 doi:10.1029/ 2009JG001102, 2010.

- 517 Frankignoulle, M., Borges, A., and Biondo, R.: A new design of equilibrator to monitor carbon dioxide
518 in highly dynamic and turbid environments, *Wat. Res.* 35(5), 1344–1347, 2001.
- 519 Fullen, M. A., Mitchell, D. J., Barton, A. P., Hocking, T. J., Liguang, L., Zhi, W. B., Yi, Z., and Yuan,
520 X.Z.: Soil erosion and Conservation in the Headwaters of the Yangtze River, Yunnan Province,
521 China, In *Headwaters: Water resources and Soil conservation*, edited by Haigh MJ, Krecke J,
522 Rajwar S, Kilmartin MP, pp. 299–306, Balkema, Rotterdam/Oxford and IBH, New Delhi, 460pp,
523 1998.
- 524 Guasch, H., Armengol, J. and Sabater, S.: Diurnal variation in dissolved oxygen and carbon dioxide in
525 two low-order streams, *Water Res.*, 32,1067–1074, 1998.
- 526 Guérin, F., Abril, G., Serça, D., Delon, C., Richard, S., Delmas, R., Tremblay, A., and Varfalvy, L.:
527 Gas transfer velocities of CO₂ and CH₄ in a tropical reservoir and its river downstream, *J. Mar.*
528 *Syst.*, 66, 161–172, 2007.
- 529 Ha, V.K., Vu, T. M. H.: Analysis of the effects of the reservoirs in the upstream Chinese section to the
530 lower section flow of the Da and Thao Rivers. *Journal of Water resources and Environmental*
531 *Engineering (in Vietnamese)* 38, 3 – 8, 2012.
- 532 Hope, D., Palmer, S.M., Billett, M.F., and Dawson, J.J.: Variations in dissolved CO and CH₄ in a first-
533 order stream and catchment: an investigation of soil-stream linkages, *Hydrol. Process.*, 18, 3255–
534 75, 2004.
- 535 Kempe, S.: Long-term records of CO₂ pressure fluctuations in freshwaters, in *Transport of Carbon and*
536 *Minerals in Major World Rivers*, edited by E. T. Degens, *Mitt. Geol. Palaont. Inst. Univ.*
537 *Hambourg*, 52, 91–332, 1982.
- 538 Lauerwald, R., Laruelle, G. G., Hartmann, J., Ciais, P., and Regnier, P. A. G.: Spatial patterns in
539 CO₂ evasion from the global river network, *Global Biogeochem. Cy.*, 29(5), 534–554,
540 DOI: 10.1002/2014GB004941, 2015.
- 541 Le, K. T.: Final report of the national project, Study on the scientific basis and practical
542 management of water supply in dry season for the Red River Delta, 2008.
- 543 Le, T. P. Q., Garnier, J., Billen, G., They, S., and Chau, V.M.: The changing flow regime and
544 sediment load of the Red River, Viet Nam, *J. Hydrol.*, 334, 199–214,
545 doi:10.1016/j.jhydrol.2006.10.020, 2007.
- 546 Le, T. P. Q., Billen, G., Garnier, J., Chau, V. M.: Long-term biogeochemical functioning of the Red
547 River (Vietnam): past and present situations, *Reg. Environ. Change.*, DOI: 10.1007/s10113-014-
548 0646-4, 2015.
- 549 Le, T. P. Q., Dao, V. N., Rochelle-Newall, E., Garnier, J., Billen, G., Lu, X. X., Echetbet, H., Duong,
550 T. T., Ho, C. T., Nguyen, T. B. N., Nguyen, B. T., Nguyen, T. M. H., Le, N. D., and Pham, Q. L.:
551 Total organic flux of the Red River system (Vietnam), *Earth. Surf. Proc. Land.*,
552 DOI: 10.1002/esp.4107, 2017.

553 Li, S., Bush, R. T.: Changing fluxes of carbon and other solutes from the Mekong River. Scientific
554 Reports 5:16005. DOI: 10.1038/srep16005, 2015.

555 Li, S., Lu, X. X., He, M., Yue, Z., Li L., and Ziegler, A. D.: Daily CO₂ partial pressure and CO₂
556 outgassing in the upper Yangtze River basin: A case study of the Longchuan River, China, J.
557 Hydrol., 466–467, 141–150, <http://dx.doi.org/10.1016/j.jhydrol.2012.08.011>, 2012.

558 Liu, S., Lu, X. X., Xia, X., Zhang, S., Ran, L., Yang, X., and Liu, T.: Dynamic biogeochemical
559 controls on river pCO₂ and recent changes under aggravating river impoundment: an example of
560 the subtropical Yangtze River. Global Biogeochemical Cycles 30 (6), 880-897, 2016.

561 Liu, S., Lu, X. X., Xia, X., Yang, X., and Ran, L.: Hydrological and geomorphological control on CO₂
562 outgassing from low-gradient large rivers: an example of the Yangtze River system. Journal of
563 Hydrology, 550, 26-41, 2017.

564 Linn, D. M. and Doran, J. W.: Effect of water-filled pore space on carbon dioxide and nitrous oxide
565 production in tilled and non- tilled soils, Soil Sci. Soc. 48(6), 1267-272, 1984.

566 Lu, X. X., Oeurng, C., Le T. P. Q., and Duong T. T.: Sediment budget as affected by construction of a
567 sequence of dams in the lower Red River, Viet Nam. Geomorphology 248, 125-133, 2015.

568 Meybeck, M., Chapman, D. V. and Helmer, R.: Global freshwater quality: a first assessment.
569 Cambridge, MA, World Health Organization/United Nations Environment Programme, Basil
570 Blackwell, Inc. 306 p, 1989.

571 Millot, R., Gaillardet, J., Dupre, B., and Allegre, C. J.: The global control of silicate weathering rates
572 and the coupling with physical erosion: new insights from rivers of the Canadian Shield, Earth
573 Planet. Sci. Lett., 196, 83–98, 2002.

574 Moacyr, A., Carlos, N., Doris, V. and Nathalie, L.: Nutrient input and CO₂ flux of a tropical coastal
575 fluvial system with high population density in the northeast region of Brazil, JWARP, 5, 362-375,
576 (2013).

577 MONRE.: Vietnamese Ministry of Environment and Natural Resources, Report Annual on
578 Hydrological Observation in Vietnam, Hanoi, 2014.

579 Moon, S., Huh, Y., Qin, J., Nguyen, V.P.: Chemical weathering in the Hong (Red) River basin: Rates
580 of silicate weathering and their controlling factors. Geochimica et Cosmochimica Acta.
581 doi:10.1016/j.gca.2006.12.004, 2007.

582 Ngo, T.T., Trinh, T.P., Luong, H.D., Kim, J.H.: Regulation effects of reservoir system on flow regime
583 in Red River downstream. Hydrology in a Changing World: Environmental and Human
584 Dimensions 1 Poster Proceedings of FRIEND-Water 2014, Hanoi, Vietnam.
585 <https://www.researchgate.net/publication/269106932>, 2014.

586 Nguyen, N. S., Hua, C. T., Nguyen, C. H., Nguyen, V. T., Lang, V. K, Pham, V. N., and Nguyen, V.
587 T.: Case study report on Red River Delta in Vietnam - Project on integrated management and
588 conservation of near shore coastal and marine areas in East Asia region (EAS-35) United Nations
589 Environment program, Regional coordinating for the East Seas (ESA/RCU), U.N. Environ.
590 Programme, Nairobi, 78pp, 1995.

591 Nguyen, T. M. H, Billen, G., Garnier, J., Le, T. P. Q, Pham, Q. L., Huon, S., Rochelle-Newall, E.,:
592 Organic carbon transfers in the subtropical Red River system (Viet Nam): insights on CO₂ sources
593 and sinks. *Biogeochemistry*. doi.org/10.1007/s10533-018-0446-x, 2018.

594 Park, P. K.: Oceanic CO₂ system: an evaluation of ten methods of investigation. *Limnol. Oceanogr.* 14,
595 179–186, 1969.

596 Parkin, T. B. and Kaspar, T. C.: Temperature controls on diurnal carbon dioxide flux, *Soil Sci. Soc.*
597 *Am. J.*, 67, 1763–1772, 2003.

598 Peter, H., Singer, G. A., Preiler, C., Chiffard, P., Steniczka, G., and Battin, T. J.: Scales and drivers of
599 temporal *p*CO₂ dynamics in an Alpine stream. *J. Geophys. Res. Biogeosciences*, 119 (6), 1078–
600 1091, doi 10.1002/2013JG002552, 2014.

601 R Core Team. R.: A language and environment for statistical computing. Vienna, Austria: R
602 Foundation for Statistical Computing, Retrieved from <https://www.rproject.org/>, 2016.

603 Ran, L., Lu, X. X., Richey, J. E., Sun, H., Han, J., Yu, R., Liao, S., and Yi, Q.: Long term spatial and
604 temporal variation of CO₂ partial pressure in the Yellow River, China, *Biogeosciences*, 12, 921–
605 932, DOI: 10.5194/bg-12-921-2015, 2015a.

606 Ran, L., Lu, X. X., Yang, H., Li, L., Yu, R., Sun, H., and Han, J.: CO₂ outgassing from the Yellow
607 River network and its implications for riverine carbon cycle. *Journal of Geophysical Research:*
608 *Biogeosciences* 120 (7), 1334–1347, 2015b.

609 Rasera M de Fatima, F.L., Krusche, A.V., Richey, J. E., Ballester, M. V. R., and Victória, R. L.: Spatial
610 and temporal variability of *p*CO₂ and CO₂ efflux in seven Amazonian Rivers, *Biogeochem.*,
611 116:241–259, doi: 10.1007/s10533-013-9854-0, 2013.

612 Raymond, P. A., and Cole, J. J.: Gas Exchange in Rivers and Estuaries: Choosing a Gas Transfer
613 Velocity, *Estuaries*, 24(2), 312–317, doi:10.2307/1352954, 2001.

614 Raymond, P. A., Caraco, N. F. and Cole, J. J.: Carbon dioxide concentration and atmospheric flux in
615 the Hudson River, *Estuaries*, 20, 381–390, 1997.

616 Raymond, P. A., Zappa, C. J., Butman, D., Bott, T. L., Potter, J., Mulholland, P., Laursen, A. E.,
617 McDowell, W.H., and Newbold, D.: Scaling the gas transfer velocity and hydraulic geometry in
618 streams and small rivers, *Limnol. Oceanogr.*, 2, 41–53, doi:10.1215/21573689-1597669, 2012.

619 Raymond, P. A., et al. : Global carbon dioxide emissions from inland waters, *Nature*, 503(7476), 355–
620 359. Doi:10.1038/nature12760, 2013.

621 Regnier, P., Friedlingstein, P., Ciais, P., Mackenzie, F. T., Gruber, N., Janssens, I. A., Laruelle, G. G.,
622 Lauerwald, R., Luyssaert, S., Andersson, A. J., Arndt, S., Arnosti, C., Borges, A. V., and Dale,
623 A.W.: Anthropogenic perturbation of the carbon fluxes from land to ocean, *Nat. Geosci.*, 6(8),
624 597–607, doi:10.1038/ngeo1830, 2013.

625 Richey, J. E., Melack, J. M., Aufdenkampe, A. K., Ballester, V. M., and Hess, L. L.: Outgassing from
626 Amazonian rivers and wetlands as a large tropical source of atmospheric CO₂, *Nature*, 416, 617–
627 620, 2002.

628 Sarma, V. V. S. S., Krishna, M. S., Rao, V. D., Viswanadham, R., Kumar, N. A. and al.: Sources and
629 sinks of CO₂ in the west coast of Bay of Bengal. *Tellus B.* 64, 10961.
630 DOI:10.3402/tellusb.v64i0.10961, 2012.

631 Sarma, V. V. S. S., Kumar, N.A., Prasad, V. R., Venkataramana, V., Appalanaidu, S. and al.: High CO₂
632 emissions from the tropical Godavari estuary (India) associated with monsoon river discharges.
633 *Geophys. Res. Lett.* 38, L08601, doi: 10.1029/2011GL046928, 2011.

634 Servais, P., Barillier, A., and Garnier, J.: Determination of the biodegradable fraction of dissolved and
635 particulate organic carbon in waters. *Int. J. Limnol.* 31(1):75-80. Doi:10.1051/limn/1995005, 1995.

636 Striegl, R. G., Dornblaser, M. M., Aiken, G. R., Wickland, K. P., and Raymond, P. A.: Carbon export
637 and cycling by the Yukon, Tanana, and Porcupine rivers, Alaska, 2001–2005, *Water Resour. Res.*,
638 43, W02411, doi:10.1029/2006WR005201, 2007.

639 Striegl, R. G., Dornblaser, M. M., McDonald, C. P., Rover, J. R., and Stets, E. G.: Carbon dioxide and
640 methane emissions from the Yukon River system, *Global Biogeochem. Cy.*, 26, GB0E05,
641 doi:10.1029/2012GB004306, 2012.

642 Telmer, K. and Veizer, J.: Carbon fluxes, *p*CO₂ and substrate weathering in a large northern river
643 basin, Canada: carbon isotope perspectives, *Chem Geol.*, 159, 61-86, 1999.

644 Trinh, A. D., Vachaud, G., Bonnet, M. P., Prieur, N., Vu, D. L., and Le, L. A.: Experimental
645 investigation and modelling approach of the impact of urban wastewater on a tropical river; a case
646 study of the Nhue River, Hanoi, Vietnam, *J. Hydrol.*, 334, 347–358, doi:10.1016/j.
647 jhydrol.2006.10.022, 2007.

648 Trinh, A. D., Giang, N. H., Vachaud, G., and Choi, S.U.: Application of excess carbon dioxide partial
649 pressure (EpCO₂) to the assessment of trophic state of surface water in the Red River Delta of
650 Vietnam, *Int. J. Environ. Stud.*, 66(1), 27–47, doi:10.1080/00207230902760473, 2009.

651 Trinh, A.D., Meysman, F., Rochelle-Newall E., and Bonnet, M. P.: Quantification of sediment-water
652 interactions in a polluted tropical river through biogeochemical modeling, *Global Biogeochem*
653 *Cy.*, 26, GB3010, doi:10.1029/2010GB003963, 2012.

654 Vinh, V.D., Ouillon, S., Thanh, T.D., Chu, L.V.: Impact of the HoaBinh dam (Vietnam) on water and
655 sediment budgets in the Red River basin and delta. *HESS.*, 18, 3987 – 4005, 2014.

656 Yao, G., Quanzhou, G., Zhengang, W., Xiakun, H., Tong, H., Yongling, Z., Shulin, J., and Jian, D.:
657 Dynamics of CO₂ partial pressure and CO₂ outgassing in the lower reaches of the Xijiang River, a
658 subtropical monsoon river in China, *Sci. Total Environ.*, 376, 255–266. DOI:
659 10.1016/j.scitotenv.2007.01.080, 2007.

660 Walling, D. E., and Fang, D.: Recent trends in the suspended sediment loads of the world's rivers,
661 *Glob. Planet. Change*, 39(1-2), 111-126, 2003.

662 Walling, D. E.: Human impact on land-ocean sediment transfer by the world's rivers, *Geomorphology*,
663 79(3-4), 192-216, 2006.

664 Wang, F., Wang, Y., Zhang, J., Xu, H., and Wei, X.: Human impact on the historical change of CO₂
665 degassing flux in the River Changjiang, *Chem. Trans.*, Doi:10.1186/1467-4866-8-7, 2007.

666 Wang, Y., Munger, J. W., Xu, S., McElroy, M. B., Hao, J., Nielsen, C. P. and Ma, H.: CO₂ and its
667 correlation with CO at a rural site near Beijing: implications for combustion efficiency in China,
668 *Atmos. Chem. Phys.*, 10, 8881–8897, doi:10.5194/acp-10-8881-2010, 2010.

669 Wang, F., Wang, B., Liu, C., Wang, Y., Guan, J., Liu, X., and Yu, Y.: Carbon dioxide emission from
670 surface water in cascade reservoirs-river system on the Maotiao River, southwest of China, *Atmos.*
671 *Environ.*, 45(23), 3827–3834, 2011.

672 Wang, Z. A., Bienvenu, D. J., Mann, P. J., Hoering, K. A., Poulsen, J. R., Spencer, R. G. M., and M.
673 Holmes R. M.: Inorganic carbon speciation and fluxes in the Congo River, *Geophys Res Lett.*, 40,
674 511–516, doi:10.1002/grl.50160, 2013.

675 Weiss, R. F.: Carbon dioxide in water and seawater: the solubility of a non ideal gas, *Mar. Chem.*, 2(3),
676 203-215, 1974.

677 Wit, F., Muller, D., Baum, A., Warneke, T., Pranowo, W. S., Muller, M. and Rixen T.: The impact of
678 disturbed peatlands on river outgassing in Southeast Asia, *Nat. Commun.* 6:10155, DOI:
679 10.1038/ncomms10155, 2015.

680

681

682

683

684 **List of tables**

685 **Table 1.** Average values (and standard deviation) of river water discharge at five hydrological stations
686 of the Red River in 2014. Data gathered from different sources (MONRE, 2014, Le, 2008)

687

688 **Table 2.** Mean values (and standard deviation) of the different physico-chemical variables at 5 sites in
689 wet and dry season in 2014.

690

691 **Table 3.** k_{600} parameterization, and calculated water-air CO_2 fluxes (mean values and standard
692 deviation) for daytime and nighttime at five hydrological stations of the Red River in dry and wet
693 seasons in 2014.

694

695 **Table 4.** Summary of the statistical analysis with the environmental variables.

696

697 Table 5. $p\text{CO}_2$ (mean value and standard deviation) from some World Rivers.

Table 1. Average values (and standard deviation) of river water discharge at five studied sites of the Red River in 2014 (MONRE, 2014; Le, 2008)

Studied sites	Altitude (m a.s.l.)	Latitude	Mean water velocity, m/s		Mean water depth, m		Mean slope	Average daily water discharge in 2014, m ³ s ⁻¹	Water discharge, m ³ s ⁻¹			
			Wet	Dry	Wet	Dry			Wet season		Dry season	
									Mean value in wet season in 2014 (May – Oct)	On the date of measurement Sept 2014	Mean value in wet season in 2014 (May – Oct)	On the date of measurement in Nov 2014
Yen Bai	56	21°42'00.0"N 104°52'00.0"E	1.0	0.9	4.8	3.7	0.0012	527 ± 515	788 ± 459	840 ± 68	262 ± 530	260 ± 18
Hoa Binh	23	20°54'00.0"N 105°21'00.0"E	0.5	0.4	11.5	9.9	0.0015	1,369 ± 833	1,907 ± 451	2,189 ± 39	825 ± 515	868 ± 319
Vu Quang	25	21°33'00"N 105°16'00"E	0.5	0.3	12.3	9.2	0.0018	1,302 ± 517	1,618 ± 378	2,240 ± 88	982 ± 284	725 ± 11
Hanoi	5	21°02'00"N 105°52'00"E	1.0	0.9	4.7	3.9	0.0012	1,867 ± 1089	2,598 ± 780	3,296 ± 86	1,127 ± 490	1,915 ± 149
Ba Lat	0	20°18'07.6"N 106°32'25.4"E	0.4	0.3	2.1	1.4	0.0003	615 ± 293	824 ± 200	1,269 ± 93	403 ± 96	453 ± 31

Table 2. Average values in day and night times of the different physico-chemical variables (average value and standard deviation) at 5 sites in wet and dry seasons in 2014.

Table 2a

Stations	Temperature °C	pH	TALK mg L ⁻¹	Salinity	Chl-a µg L ⁻¹	Turbidity NTU	Conductivity mS cm ⁻¹	DOC mg L ⁻¹	POC mg L ⁻¹	DO %	Measured pCO ₂ ppm	Calculated pCO ₂ ppm
Wet season												
<i>1-Yen Bai</i>												
Day	26.4±0.1	8.2±0.1	105.1±5.2	0.1±0.0	3.1±0.1	141.6±8.6	0.2±0.0	1.5±0.2	2.1±0.4	69.9±0.2	963.9±9.4	699.1±86.1
Night	26.6±0.0	8.3±0.0	103.8±3.3	0.1±0.0	3.1±0.1	135.4±4.0	0.2±0.0	1.4±0.2	1.9±0.2	70.4±0.1	981.3±7.7	609.1±26.5
<i>2-Vu Quang</i>												
Day	26.8±0.1	8.1±0.0	148.9±6.7	0.1±0.0	1.2±0.2	51.4±7.5	0.2±0.0	1.1±0.3	1.4±0.2	63.6±1.2	1598.7±53.3	1169.2±131.2
Night	27.0±0.1	8.2±0.0	144.9±3.3	0.1±0.0	1.2±0.2	49.9±5.3	0.2±0.0	1.0±0.2	1.4±0.2	63.2±0.7	1583.0±36.6	1058.5±33.0
<i>3-Hoa Binh</i>												
Day	26.5±0.1	7.8±0.0	110.4±3.3	0.1±0.0	0.8±0.3	42.5±4.7	0.2±0.0	1.5±0.4	1.1±0.2	54.9±0.2	3827.1±60.6	2125.9±294.5
Night	26.4±0.0	7.8±0.0	107.8±5.4	0.1±0.0	1.2±0.0	41.0±0.1	0.2±0.0	1.3±0.2	1.1±0.1	55.1±0.6	3830.2±19.1	1747.0±56.8
<i>4-Ha Noi</i>												
Day	28.6±0.2	8.0±0.0	84.3±1.9	0.1±0.0	2.0±0.6	88.9±1.3	0.2±0.0	4.7±0.6	2.0±0.3	64.0±0.4	1412.6±4.0	888.7±108.3
Night	28.6±0.2	8.1±0.0	84.5±1.5	0.1±0.0	2.7±0.1	88.5±2.7	0.2±0.0	4.2±0.9	2.2±0.4	63.5±0.3	1411.0±7.0	768.6±47.3
<i>5-Ba Lat</i>												
Day	28.9±0.4	8.0±0.1	116.4±4.6	0.3±0.3	1.8±0.3	47.7±8.8	0.6±0.6	1.5±0.4	1.1±0.2	66.1±1.4	1499.2±103.2	1312.2±267.3
Night	28.8±0.3	8.1±0.0	114.9±3.5	0.1±0.1	2.5±0.1	81.3±10.0	0.3±0.2	1.7±0.5	1.5±0.2	65.1±1.6	1471.3±118.1	1156.7±77.6

Table 2b

Stations	Temperature °C	pH	TALK mg L ⁻¹	Salinity	Chl-a µg L ⁻¹	Turbidity NTU	Conductivity mS cm ⁻¹	DOC mg L ⁻¹	POC mg L ⁻¹	DO %	Measured pCO ₂ ppm	Calculated pCO ₂ ppm
Dry season												
<i>1-Yen Bai</i>												
Day	24.1±0.5	8.1±0.1	113.9±7.9	0.1±0.0	1.2±0.3	49.3±7.9	0.2±0.0	1.3±0.3	1.4±0.1	69.3±0.7	995.8±17.5	896.8±320.3
Night	24.2±0.3	8.2±0.0	109.3±2.8	0.1±0.0	1.6±0.2	42.5±4.7	0.2±0.0	1.2±0.2	1.2±0.3	69.1±0.5	1030.6±21.5	655.0±19.5
<i>2-Vu Quang</i>												
Day	24.7±0.2	8.3±0.0	134.9±5.1	0.1±0.0	1.0±0.2	28.1±1.7	0.2±0.0	1.1±0.2	1.1±0.2	67.0±0.9	1235.3±76.2	756.2±81.7
Night	24.8±0.4	8.4±0.0	129.3±2.7	0.1±0.0	1.4±0.2	32.4±3.7	0.2±0.0	1.1±0.2	1.2±0.1	69.0±0.9	1163.3±86.3	604.2±35.0
<i>3-Hoa Binh</i>												
Day	26.3±0.0	7.8±0.0	122.5±6.1	0.1±0.0	0.5±0.1	16.9±0.3	0.2±0.0	0.9±0.2	0.5±0.1	51.5±0.4	2399.3±33.6	2091.7±227.2
Night	26.3±0.0	7.8±0.0	120.6±6.1	0.1±0.0	0.5±0.1	17.1±0.5	0.2±0.0	0.9±0.2	0.5±0.1	51.3±0.2	2458.9±14.0	2003.9±200.7
<i>4-Ha Noi</i>												
Day	23.8±0.1	8.2±0.0	123.5±2.4	0.1±0.0	1.7±0.2	65.2±1.8	0.2±0.0	2.7±0.7	1.5±0.3	66.8±0.4	1141.3±33.5	797.7±95.4
Night	23.8±0.1	8.3±0.0	123.8±1.5	0.1±0.0	1.6±0.1	62.6±0.7	0.2±0.0	2.0±0.7	1.3±0.1	67.1±0.3	1136.0±24.2	726.1±5.9
<i>5-Ba Lat</i>												
Day	23.7±0.1	8.3±0.0	152.9±6.6	3.9±2.4	1.8±0.2	34.1±8.3	6.6±3.4	1.4±0.2	2.0±0.4	70.0±0.5	751.4±49.3	753.6±56.5
Night	23.4±0.1	8.3±0.0	150.3±5.6	3.3±1.6	1.3±0.2	28.8±4.2	5.7±2.6	1.2±0.2	1.9±0.4	68.8±0.6	881.0±88.4	795.1±46.3

Table 3. k_{600} parameterization, and calculated water-air CO₂ fluxes for day time and night time at five hydrological stations of the Red River in dry and wet seasons in 2014.

	Wind speed m s ⁻¹	k_{600} cm h ⁻¹	Water-air CO ₂ flux, mmol m ⁻² d ⁻¹ (with $p\text{CO}_2$ measured from equilibrator)
Wet season			
Yen Bai			
Day	1.1±0.6	66.1±0.55	304.5±3.9
Night	0.5±0.6	66.5±0.09	315.2±4.0
Vu Quang			
Day	0.9±0.7	84.2±0.12	824.0±36.7
Night	0.4±0.6	84.1±0.02	811.8±25.1
Hoa Binh			
Day	1.3±1.1	69.1±0.27	1935.2±38.3
Night	0.2±0.5	69.0±0.03	1931.3±10.0
Hanoi			
Day	1.8±0.7	54.0±0.96	446.6±8.7
Night	1.2±0.6	53.5±0.17	441.6±3.6
Ba Lat			
Day	0.5±0.5	9.1±0.05	81.1±7.8
Night	0.2±0.3	9.1±0.02	79.4±8.6
Dry season			
1-Yen Bai			
Day	1.4±0.9	59.6±0.72	290.5±8.2
Night	0.5±0.8	60.1±0.54	309.3±13.3
2-Vu Quang			
Day	1.3±0.6	52.4±0.11	356.6±33.0
Night	0.7±1.3	52.4±0.15	326.3±37.0
3- Hoa Binh			
Day	1.2±0.8	58.4±2.85	938.4±22.7
Night	0.5±0.5	58.5±1.97	985.0±38.6

4-Hanoi			
Day	2.4±0.5	47.4±0.60	287.0±16.2
Night	1.4±0.5	47.3±0.57	284.2±12.7
5-Ba Lat			
Day	3.1±1.5	8.6±0.07	24.7±3.5
Night	1.3±0.8	8.5±0.03	33.5±6.1

5

10

15

Table 4. Relationship between $p\text{CO}_2$ and $f\text{CO}_2$ with other water quality variables

	Temp, °C	DOC, mg.L ⁻¹	POC, mg.L ⁻¹	Talk, mg L ⁻¹	$p\text{CO}_2$, ppm	pH	DO, mg.L ⁻¹	Sal, %	Chl_a, µgL ⁻¹	DO, %	Turb., NTU	Conduct., mScm ⁻¹	River Flow, m ³ .s ⁻¹	$f\text{CO}_2$, mmol.m ⁻² .d ⁻¹
Temp, °C	1													
DOC, mg.L ⁻¹	0.29	1.00												
POC, mg.L ⁻¹	0.00	0.36	1.00											
Talk, mg L ⁻¹	-0.47	-0.52	-0.08	1.00										
$p\text{CO}_2$, ppm	0.31	-0.14	-0.64	-0.15	1.00									
pH	-0.50	0.01	0.60	0.28	-0.85	1.00								
DO conc, mg.L ⁻¹	-0.58	0.02	0.62	0.18	-0.83	0.91	1.00							
Sal, %	-0.37	-0.08	0.30	0.50	-0.26	0.31	0.33	1.00						
Chl_a, µgL ⁻¹	0.30	0.32	0.66	-0.46	-0.48	0.41	0.43	0.02	1.00					
DO, %	-0.33	0.12	0.71	0.05	-0.86	0.89	0.96	0.25	0.60	1.00				
Turb., NTU	0.34	0.33	0.57	-0.56	-0.33	0.25	0.27	-0.23	0.87	0.44	1.00			
Conduct., mScm ⁻¹	-0.38	-0.08	0.32	0.51	-0.27	0.32	0.34	0.99	0.02	0.25	-0.23	1.00		
River Flow, m ³ .s ⁻¹	0.53	0.57	0.10	-0.33	0.36	-0.34	-0.44	-0.30	0.07	-0.33	0.18	-0.31	1.00	
$f\text{CO}_2$, mmol.m ⁻² .d ⁻¹	0.21	-0.16	-0.56	-0.12	0.95	-0.75	-0.75	-0.28	-0.48	-0.79	-0.27	-0.29	0.38	1

Table 5. $p\text{CO}_2$ (average value and standard deviation) of some World Rivers.

River or Tributary	Location	Country	Mean $p\text{CO}_2$ ppm	F_{CO_2} mmol m^{-2} day^{-1}	$k600 \pm \text{SD}$ cm h^{-1}	References
Red		Vietnam	$1,589 \pm 43$	550.3 ± 16.9	50.9 ± 27	This study
Mekong	Downstream	Laos and Cambodia	703 – 1597	88.1 - 378.4	12.4 - 44.5	<i>Alin et al., 2011</i>
Tonle Sap	Stung Siem Reap	Cambodia	3,067	139.1	5.6 ± 0.9	<i>Alin et al., 2011</i>
Tonle Sap	Pousat River	Cambodia	1,404	98.5	10.8 ± 2.8	<i>Alin et al., 2011</i>
Musi		Indonesia	$4,317 \pm 928$	5 ± 1.1	21.8 ± 4.7	<i>Wit et al., 2015</i>
Batanghari		Indonesia	$2,401 \pm 18$	1.8 ± 0.4	21.8 ± 4.7	<i>Wit et al., 2015</i>
Indragiri		Indonesia	$5,779 \pm 527$	9.7 ± 2.2	21.8 ± 4.7	<i>Wit et al., 2015</i>
Siak		Indonesia	$8,557 \pm 528$	8.3 ± 1.9	22.0 ± 4.7	<i>Wit et al., 2015</i>
Lupar		Malaysia	$1,274 \pm 148$	13 ± 3.0	26.5 ± 9.3	<i>Wit et al., 2015</i>
Saribas		Malaysia	$1,159 \pm 29$	14.6 ± 3.3	17.0 ± 13.6	<i>Wit et al., 2015</i>
Changjiang		China	$1,297 \pm 901$	143	8 - 15	<i>Wang et al., 2007</i>
Maotiao		China	3741	108	10	<i>Wang et al. 2011</i>
Longchuan		China	2,101	156	8	<i>Li et al., 2012</i>
Yellow		China	$2,811 \pm 1,986$	856 ± 409	42.1 ± 16.9	<i>Ran et al., 2015</i>
Xijiang		China	600 - 7200	160-357	15	<i>Yao et al., 2007</i>
Krishna		India	$17,210 \pm 3501$		nd	<i>Sarma et al.,</i>

Godavari		49,832±1042			2012
Mahanadi		95,884±2235			
Ganges		5,030±100			
Gaderu Creek	India	2,216 ± 864a	56.0 ± 100.9	4 ± 5	<i>Borges et al., 2003</i>
Rhone	France	2,016±944	nd	15	<i>Cole et al., 2001</i>
Hudson	USA	1,125±403	nd	4.1	<i>Raymond et al., 1997</i>
Ottawa	Canada	1,200	80.8	4	<i>Telmer and Veizer, 1999</i>
Amazon		4,351 ± 1900	190 ± 55	9.6 ± 3.8	<i>Richey et al., 2002</i>
Mississippi		100 - 600	270	3.9	<i>Dubois et al., 2010; Lohrenz and Cai, 2006</i>
Nagada Creek	The northern Papua New Guinea coast	799 ± 357	43.6 ± 33.2	8 ± 6	<i>Borges et al., 2003</i>
Negro		3,011±304	534±148	20.3±7.6	
Solimoes		5,685±464	488±83	7.3±2.4	
Arguaia	South America	1,012±309	153±44	8.4±2.4	<i>Rasera et al., 2013</i>
Javaes		1,673±273	108±34	7.2±2.7	
Caxiuana		3,216±496	335±61	11.3±3.5	

Teles Pires			1,419±224	100±27	10.1±1.5	
Cristalino			1,938±201	202±31	15.7±2.2	
	Upper	North America	1,220 ± 9	6	1.25	
Yukon	Middle		1,890 ± 10	62	7.92	<i>Striegl et al., 2007; 2012</i>
	Lower		3,091 ± 17	193	15	
Congo			2019 - 6855	298.6	9.3 – 10.3	<i>Wang et al., 2013</i>

^a calculated the values for the $p\text{CO}_2$ Water-Air Gradient ($p\text{CO}_2$ in ppm)

nd. No data

List of figures

Figure 1: The Red River system and sampling sites (hydrological station).

5 **Figure 2.** Comparison the results of riverine $p\text{CO}_2$ and $f\text{CO}_2$ at 5 sites studied of the lower Red River by the measured (equilibrator) and calculated (CO2_SYS) methods

Figure 3 Spatial and seasonal variation of CO_2 flux out-gassing in the Red River system in 2014.

10

Figure 4: 4a: Seasonal variation of different variables at 5 sites of the lower Red River in dry (Nov) and wet (Sept) seasons in 2014

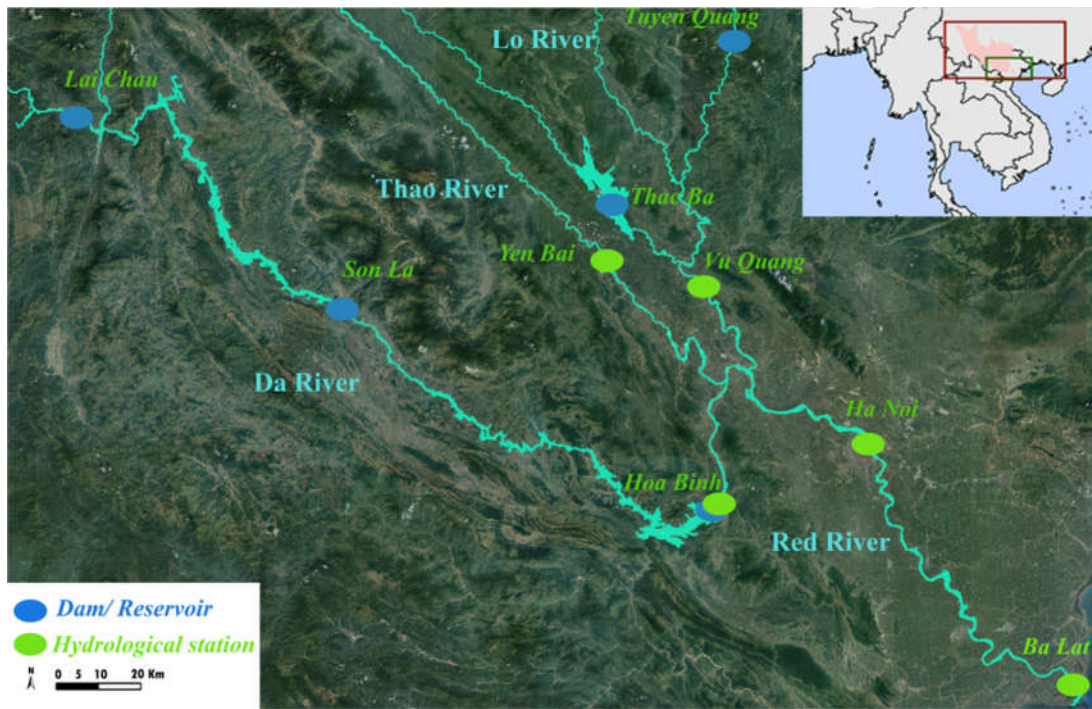
4b: Spatial variation of different variables at 5 sites of the lower Red River in dry and wet season in 2014

15

Figure 5 Relationship between $p\text{CO}_2$ - water temperature and $f\text{CO}_2$ - water temperature at 5 sites observed of the lower Red River in dry season in 2014.

20

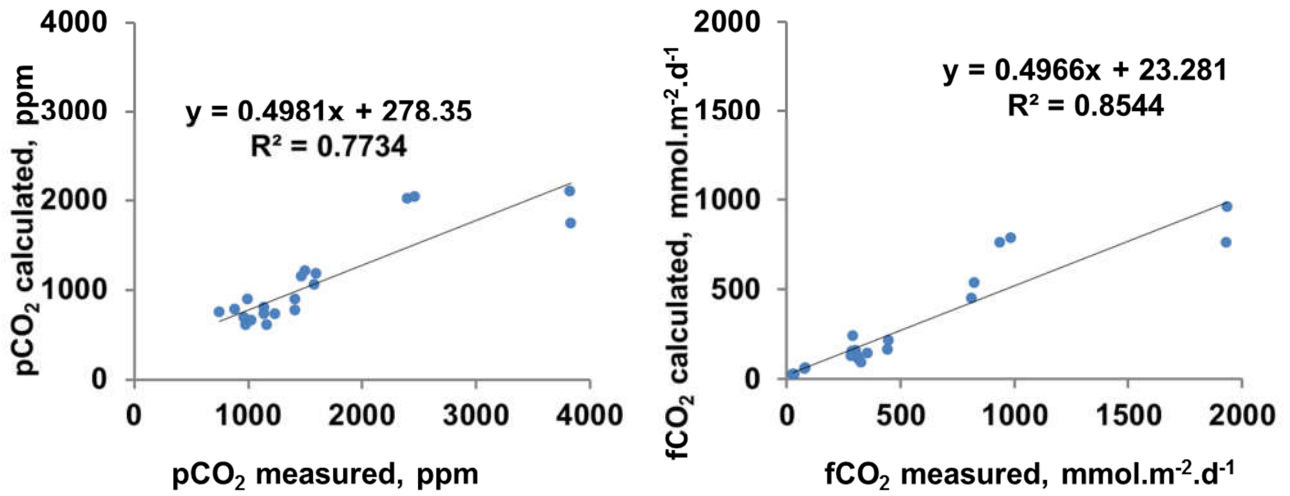
25



5

Figure 1. The Red River system and sampling sites (hydrological stations)

10



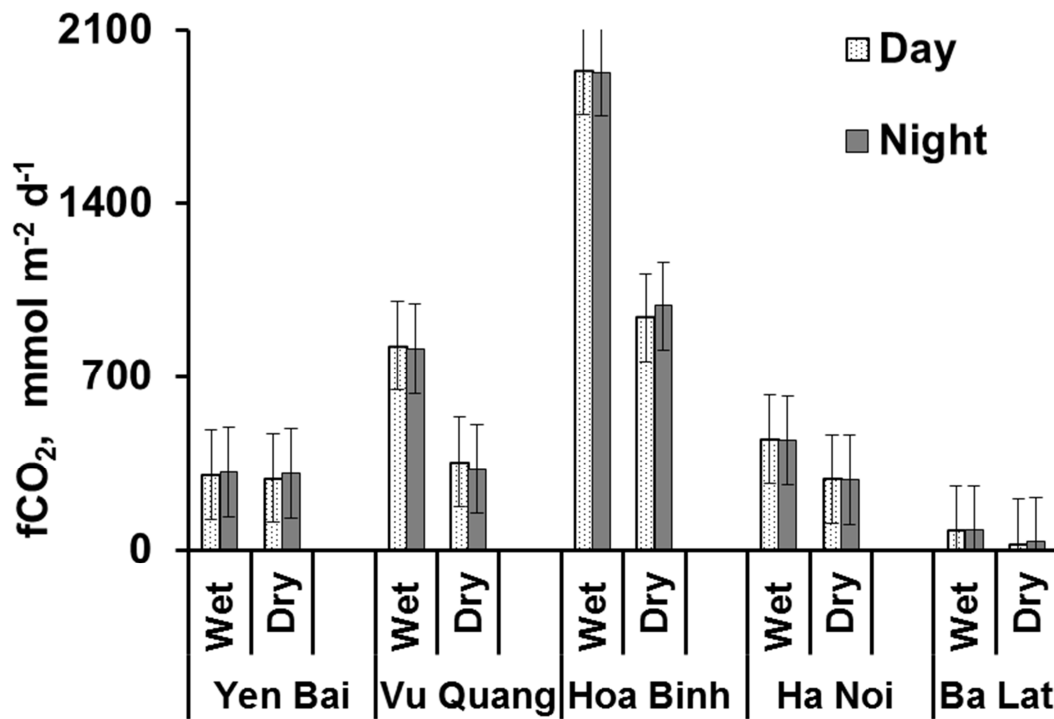
5

Figure 2. Comparison the results of riverine *p*CO₂ and *f*CO₂ at 5 sites studied of the lower Red River by the measured (equilibrator) and calculated (CO₂_SYS) methods

10

15

20

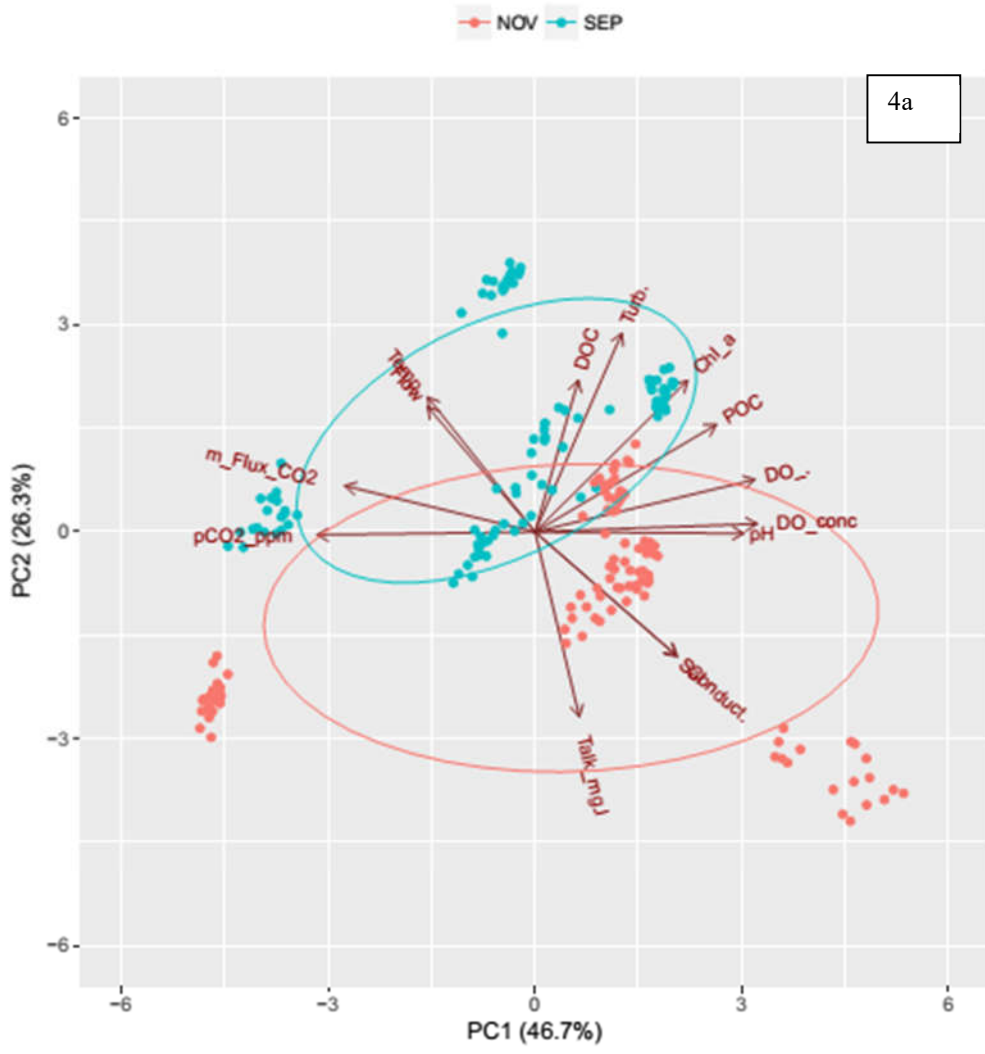


5

Figure 3 Spatial and seasonal variation of CO₂ out-gassing flux in the Red River system in 2014.

10

15



4a

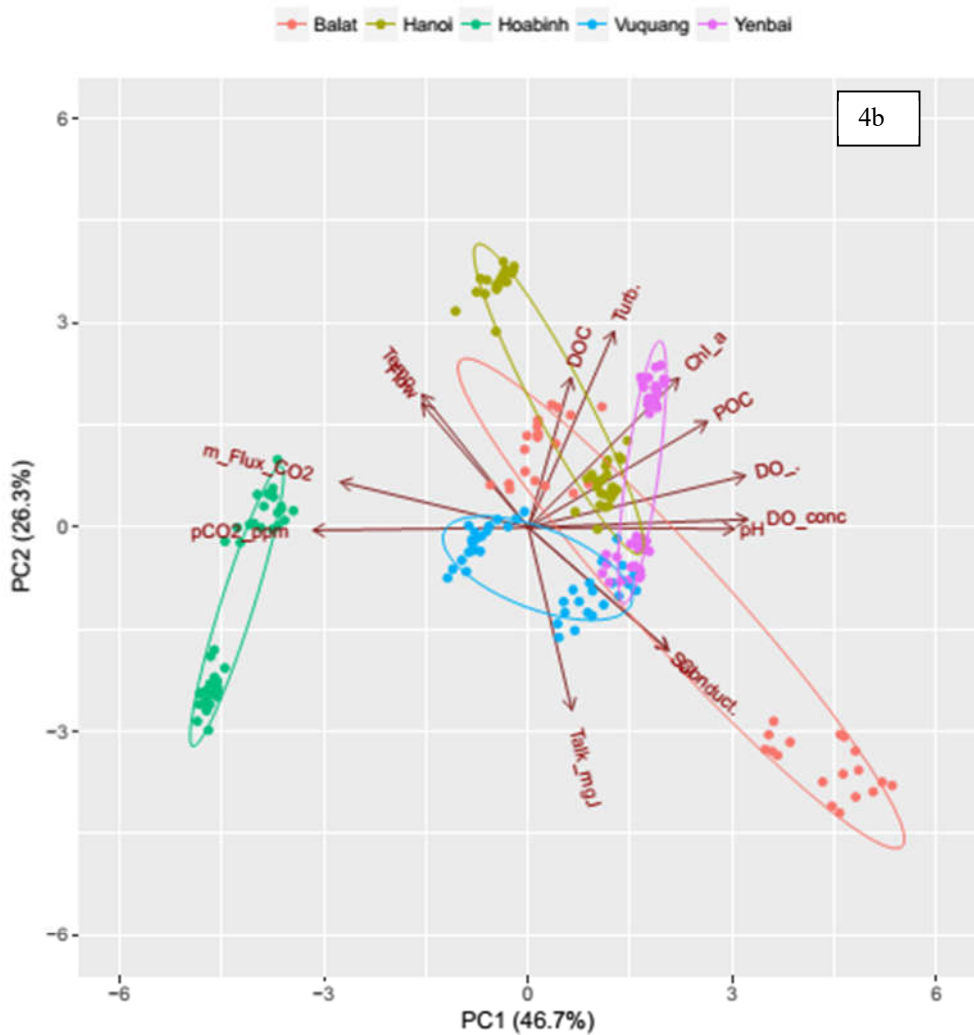


Figure 4.

- 5 4a: Seasonal variation of different variables at 5 sites of the lower Red River in dry (Nov) and wet (Sept) seasons in 2014
- 4b: Spatial variation of different variables at 5 sites of the lower Red River in dry and wet season in 2014

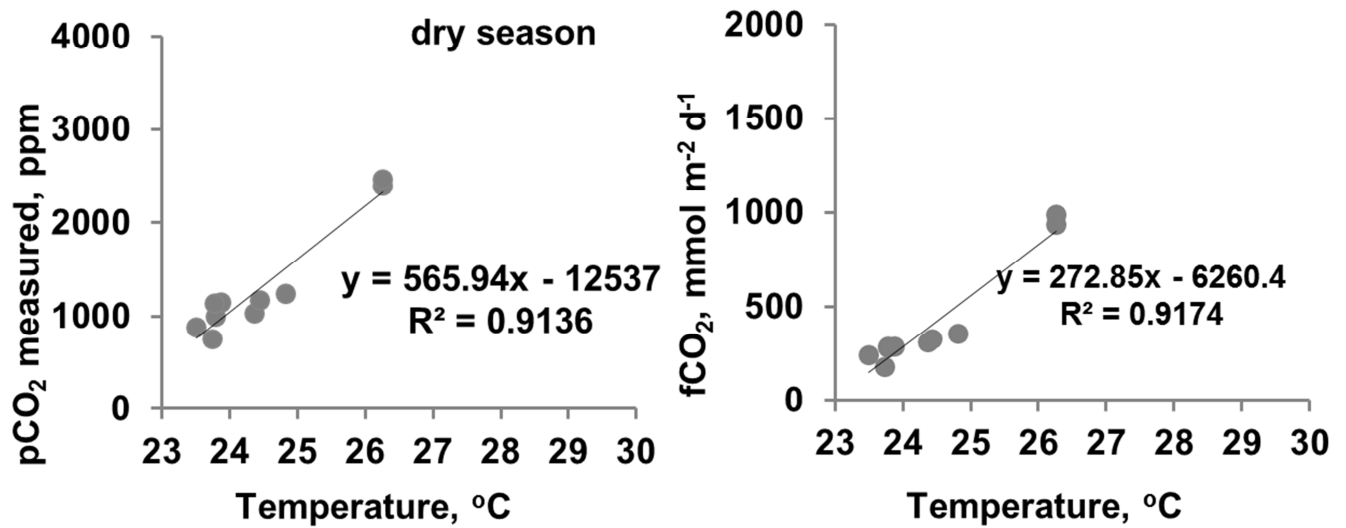


Figure 5. Relationship between $p\text{CO}_2$ -water temperature and $f\text{CO}_2$ -water temperature at 5 sites observed of the lower Red River in dry season in 2014.